

Application of Chemiluminescence to Probe Miscibility in Metallocene-Catalyzed Polyethylene Blends

Marlene J. Cran,¹ Peter K. Fearon,² Norman C. Billingham,² Stephen W. Bigger¹

¹*School of Molecular Sciences, Victoria University of Technology, P.O. Box 14428, Melbourne City Mail Centre, Melbourne, 8001, Australia*

²*School of Chemistry, Physics and Environmental Science, University of Sussex, Falmer, Brighton, BN1 9QJ, United Kingdom*

Received 30 May 2002; accepted 12 November 2002

ABSTRACT: Chemiluminescence (CL) monitoring has successfully been applied to the study of the oxidative degradation of two-component polyethylene blends made with commercially available low-density polyethylene, linear low-density polyethylene, high-density polyethylene, and metallocene-catalyzed linear low-density polyethylene (mLLDPE) formulations. The emphasis in the analysis of the results is placed on blends containing mLLDPE to address the lack of CL information on these blends. The CL data are consistent with the thermal and physicomechanical properties of the blends, with a decreased blend miscibility being reflected in the CL data as a departure from the idealized

behavior observed for more miscible blends. Furthermore, the results suggest that immiscibility in the solid state is reflected to some extent in the behavior of the melt. Preliminary experiments conducted to determine the level of consistency of CL results with respect to both variability between instruments and variability between techniques indicate a high degree of correlation in each case. © 2003 Wiley Periodicals, Inc. *J Appl Polym Sci* 89: 3006–3015, 2003

Key words: blends; luminescence; metallocene catalysts; polyethylene (PE); stabilization

INTRODUCTION

The thermooxidative stability of a polymer is an important consideration, particularly during its melt processing, during which excessive degradation can adversely affect its ultimate properties and thereby reduce its service life. Therefore, most commercial polymer formulations contain some antioxidant (AO) to inhibit degradation during processing. At low temperatures, the thermal stability of polyethylene (PE) is affected mainly by the presence of trace metals or acid residues that originate from the polymerization process.¹ At high temperatures, such as those required for melt processing, the stability of PE is influenced mainly by the presence of unsaturated sites in its structure that can result in chain branching and breakage.¹

The solid-state thermooxidative degradation of low-density polyethylene (LDPE) film^{2–5} is believed to occur homogeneously as long as the film thickness is kept constant.³ In some cases, heterogeneous oxidation is observed in which the oxidation spreads from oxidized amorphous regions to unoxidized amor-

phous regions in the polymer. A model has been proposed to account for the heterogeneous oxidation process and has been applied to the thermooxidative degradation of high-density polyethylene (HDPE) and linear low-density polyethylene (LLDPE).^{4,5} The difference between the oxidative stabilities of these polymers is attributed to their different crystallinities as well as the presence of less stable tertiary carbons in LLDPE.⁶ In particular, HDPE has been reported to exhibit a lower rate of oxidation than LLDPE, with catalyst residues influencing its rate of oxidation more than the crystallinity.⁶

As metallocene-catalyzed linear low-density polyethylene (mLLDPE) has a low degree of unsaturation and a low level of metal residues, it should exhibit a high intrinsic oxidative stability.¹ Indeed, the thermooxidative stabilities of various types of PE have been reported to decrease in the order HDPE > mLLDPE > LLDPE,⁷ which is also in agreement with the findings of Foster et al.¹ However, a study⁸ of the thermomechanical degradation of different PEs during processing suggests that conventional LLDPE is more stable than mLLDPE; this is contrary to the previous findings.¹ It is apparent that the current literature contains some inconsistencies with respect to the relative stabilities of the different types of PEs.

The thermooxidative stability of polymer blends is becoming an important topic, as blending is now a widely used method of producing materials with tai-

Correspondence to: S. W. Bigger (stephen.bigger@vu.edu.au).

Contract grant sponsor: Pirelli Cables, Ltd.

lored properties. The thermooxidative stability of a blend may be affected by factors such as the processing conditions,⁹ the choice of vulcanizing system¹⁰ in the case of vulcanized blends, the extent of crosslinking,¹¹ and the chemical nature of the components in the blend. For example, blends of ethylene vinyl acetate polymer with LDPE exhibit higher thermal stabilities than either of the pure constituents, and this has been attributed to the effects of crosslinking.¹¹ Moreover, the blending of LDPE and isotactic polypropylene (iPP) is reported to increase the oxidative stability of the latter, presumably because of the dilution of tertiary alkyl radicals of iPP by the domains of LDPE.¹²

The development of chemiluminescence (CL) monitoring has resulted in a reliable technique for determining the oxidative stability of polymer formulations.^{13–19} CL may be observed when a polymer such as a polyolefin is heated in the presence of oxygen,¹⁹ and CL is believed to originate from excited-state carbonyl groups formed during the termination step in the autoxidative process.²⁰ The chemiluminescence oxidative induction time (CL-OIt) derived from single-photon-counting CL experiments is a measure of polymer stability and is obtained by the monitoring of the intensity of CL emission as a function of time during polymer oxidation. The CL-OIt is the time corresponding to the point of intersection between the extended baseline and the extrapolated, integrated CL signal obtained during steady-state autoxidation.¹⁹ More recently, chemiluminescence imaging (CLI)^{21–23} has been developed, and this technique shows considerable potential as a reliable method for simultaneously collecting the CL emission from multiple samples.²⁴ An oxidative induction time (OIt) can also be derived from CLI experiments (CLI-OIt). CL monitoring is regarded as a highly sensitive technique that often gives greater baseline stability over long induction times than methods such as differential scanning calorimetry (DSC).²⁵

A number of CL studies for a range of polyolefins have reported the relative thermooxidative stabilities of the polymers. For example, in an early study, Audouin-Jirakova and Verdu²⁶ found that the stability of certain polyolefins decreased in the following order: HDPE > LDPE > ethylene/propylene copolymer > polypropylene (PP). This order was also found to correspond to an increasing degree of branching among the polymers. Indeed, it has been suggested²⁷ that the intensity of CL emission from LLDPE depends on the type and degree of short-chain branching (SCB), with longer, more frequent SCB producing a higher CL intensity than shorter, less frequent SCB. In other CL studies, a decreasing order of stability of HDPE > LLDPE > LDPE > iPP has been reported for additive-free polyolefins,²⁸ and a decreasing order of HDPE > poly(4-methylpentene) > iPP > polybutene

has also been reported.²⁹ In a further study, a good correlation has been found between the CL-OIt and physicomechanical properties of multiextruded PP.¹⁶ A comparison of the stabilities of PE materials, as assessed by different experimental methods, is summarized in Table I.

The application of CL techniques to the study of polymer blends has received relatively little attention in the literature to date.^{14,15,30,31} Nonetheless, in the study of polymer blends, CL monitoring techniques have the potential to reveal important aspects, such as the stability of the blend and blend miscibility, that may subsequently lead to the development of more compatible blends. For example, in a study of the oxidative stability of poly(2,6-dimethyl-*p*-phenylene ether) in blends with polystyrene (PS) and polybutadiene (PBD), CL has been used successfully to develop optimized stabilizing conditions for the system.¹⁵ In another study, compatible mixtures of PS with poly(vinyl methyl ether) studied by CL show that at temperatures at which phase separation occurs, the luminescence is stronger than that emitted from a homogeneous blend.³⁰ In recent studies, blends of LDPE with natural rubber (NR) or styrene-butadiene rubber (SBR) studied by CL reveal that the rate of oxidation is faster in LDPE/NR blends than LDPE/SBR blends.¹⁴ Furthermore, the technique of second time derivative (STD) analysis of CL profiles was successfully applied to a 5% (w/w) blend of PBD and PP, and enabled the oxidations of the separate phases to be elucidated.³¹

The application of CL techniques to polyolefin blends may offer new insights into the thermooxidative stability of these materials. In this article, the application of CL monitoring techniques to PE blends is examined to identify any possible relationship between CL-OIt data and various physicomechanical properties of the blends. An emphasis is placed on metallocene-catalyzed PEs to partly address this lack of published information on such systems. In addition to this, particular attention is directed to the assertion that any incompatibility reflected in the physicomechanical properties of a given blend system is also reflected in the CL behavior of that system. The relative stabilities of the pure components and the performance of commercial stabilizers in the blends are also reported along with data obtained from CLI experiments that enable a preliminary assessment to be made of the reproducibility of the CL technique.

EXPERIMENTAL

Materials

The resins used to prepare the blends were commercially available PE resins. With the exception of LDPE1 and LDPE2, the resins contained chemically equivalent commercial phenolic AOs. The characteristics of

TABLE I
Comparison of the Stabilities of PE Materials as assessed by Different Experimental Methods

Analysis method	Decreasing order of stability	Comments	Reference
Thermooxidative degradation			
Carbonyl	LLDPE > mLLDPE > HDPE	Order in agreement with ref. 1	7
Thermogravimetric	mLLDPE > HDPE > LLDPE		7
Hydroperoxide	mLLDPE > LLDPE > HDPE	Catalyst residue in mLLDPE may decompose POOH	7
Various	mLLDPE > LLDPE > LDPE	mLLDPE has low unsaturation and low residue levels	1
Chemiluminescence	HDPE > LLDPE > LDPE > iPP	HDPE has low unsaturation and branching LLDPE has higher purity and regularity than LDPE CL increases with increased branching	28
Carbonyl	HDPE > LDPE > EP > PP	Order reflects increased branching	26
	HDPE > P4MP > iPP > PB	Order reflects increased branching	29
	HDPE > LLDPE	Catalyst residues affect oxidation more than crystallinity	6
Carbonyl	HDPE/LDPE blends > HDPE, LDPE	Blends less sensitive to oxidation than pure components	45
Thermomechanical degradation			
Various	HDPE > LDPE > LLDPE > mLLDPE	Stability of LLDPE is preserved by the addition of AO Adding AO to mLLDPE does not retard degradation	8
Thermogravimetric	stable iPP > unstable LDPE > 1:1 blend	LDPE dilutes 3° alkyl radicals of iPP in LDPE domains	12

EP = ethylene-propylene copolymer.
P4MP = poly-4-methylpentene.

the polymers are shown in Table II, and the various blend systems are defined in Table III.

Blend preparation

Before film extrusion, the components of the B1 and B3 blends were dry-blended for 15 min. Film samples of each blend were prepared with a Gloucester film extruder (Gloucester, MA) with the following average conditions: melt temperature = 190°C, frost height = 400 mm, screw speed = 70 rpm, gauge width = 45 mm and die gap ~ 1.5 mm. Each B2 and B4 blend was prepared by the melt compounding of the polymers in a Werner

and Pfliederer twin-screw extruder (Stuttgart, Germany) at 190°C with an average screw speed of 120 rpm. The B2 and B4 blends were compression-molded to a thickness of 2 mm in accordance with ASTM method D 1894-90. For CL and DSC measurements, plaques (100 μm thick) of the blends were prepared by compression molding at 180°C and 0.5 MPa and were immediately quenched by immersion in cold water.

Property measurements

The mechanical properties of the B1 and B3 blends were measured on film samples, whereas those of the

TABLE II
Characteristic Properties of the Polymers Used for the Blends

PE	Comonomer	MI ₂ (dg min ⁻¹)	Density (g mL ⁻¹)	AO level (ppm)
LDPE1		0.2	0.921	0
LDPE2		73	0.918	0
HDPE1		0.1	0.954	300
HDPE2		0.9	0.956	500
LLDPE	Hexene	0.7	0.921	500
mLLDPE1	Hexene	1.1	0.917	1000
mLLDPE2	Butene	28	0.901	250
mLLDPE3	Butene	34	0.882	250
mLLDPE4	Octene	1.1	0.897	1000

HDPE1 was produced by slurry polymerization; HDPE2 was produced by gas-phase polymerization.

TABLE III
Systems of the Blends that Were Studied

	LDPE1	LDPE2	mLLDPE1	mLLDPE4
LLDPE	B1(a)		B3	
mLLDPE1	B1(b)			
mLLDPE2		B2(a)		
mLLDPE3		B2(b)		
HDPE1				B4(a)
HDPE2				B4(b)

B2 and B4 blends were determined with pressed plaques. Melt-flow index (MI_2) and the density were measured in accordance with ASTM methods D 1238-98 and D 792-98, respectively. The concentration of phenolic AO was measured with ASTM methods D 5815-96, D 1996-97, and D 5524-96. The DSC melting endotherm of each blend was recorded in accordance with ASTM method D 3417-83 with a PerkinElmer DSC-7 differential scanning calorimeter (Shelton, CT). The dart impact resistance of each B1 and B3 film blend samples was determined in accordance with ASTM method D 1709-98. The tensile testing of the B2 blends was conducted in accordance with ASTM method D 638-98, and the Izod pendulum impact strength testing of the B4 blends was measured with ASTM method D 256-00.

Each of these physicomechanical tests was performed on samples from each of the blend systems. The selection of tests encompasses fast-rate, large-deformation tests such as dart impact strength and Izod impact strength as well as slow-rate, small-deformation tests such as tensile yield strength. A considerable degree of consistency was found among the results obtained across the range of physicomechanical tests for a given blend system. Certainly, the physicomechanical test results enabled each blend system to be generally classified as exhibiting ideal or nonidealized behavior. The results of typical physicomechanical tests are presented in this article. These results reflect the general behavior of a given blend system as revealed by the entire suite of physicomechanical tests that were performed and have been chosen to represent the diversity of the selection of tests.

CL recorded by photon counting

Two different photon-counting apparatus were used to collect the CL data. Each instrument contained a quartz-fronted bi-alkali cathode photomultiplier tube (model 9813-QB, Thorn-EMI, Middlesex, United Kingdom) coupled to a single-gated photon counter (model SR400, Stanford Research Systems, Sunnyvale, CA). The signal-to-noise ratio was maintained at a high level by the cooling of the photocathode to -20°C during the experiments. In one of the instruments (CL instrument #1), a Eurotherm model 2416 controller

(Worthing, West Sussex, UK) was used to maintain the sample at a constant temperature. In the other instrument (CL instrument #2), the specimen was contained in the sample compartment of a Mettler model 821^e DSC instrument (Mettler Toledo, Greifensee, Switzerland). All CL experiments were carried out at 170°C in an oxygen atmosphere (1 bar; flow rate = 100 mL min^{-1}).

CL recorded by imaging

The CL of the oxidizing polymer was recorded with a charged coupling device (CCD) camera (TE3/W/S, Astrocam, Perkin Elmer Optoelectronics GmbH, Wiesbaden, Germany), and the sample was oxidized on the temperature-controlled hot stage of a DSC instrument (821^e DSC, Mettler) that could be connected to either an oxygen or nitrogen supply. The CCD chip of the camera was kept at -40°C during the experiments.

STD analysis

All raw CL data obtained either from the single-photon-counting experiments or the CLI experiments were subjected to STD analysis³¹ to derive accurate values of the CL-OIt and CLI-OIt.

RESULTS AND DISCUSSION

Idealized systems

Figure 1 shows typical DSC traces for selected blends belonging to the B1(b) system (i.e., blends featuring mLLDPE1 as one of the components) on the first heating after quench cooling. In each case, a single endotherm is observed, which suggests that the blends are melt-miscible and compatible on a molecular level.^{32,33} Similar behavior is also observed for blends within the B1(a) system. As a result, one may expect that the physicomechanical properties and oxidative stability of the B1(a) and B1(b) systems will exhibit idealized

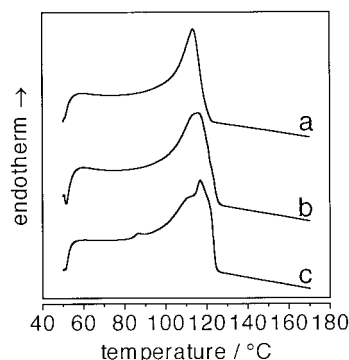


Figure 1 DSC endotherms of selected blends belonging to the B1(b) system. The blends contained (a) 20, (b) 40, and (c) 70% (w/w) mLLDPE1 in LDPE1.

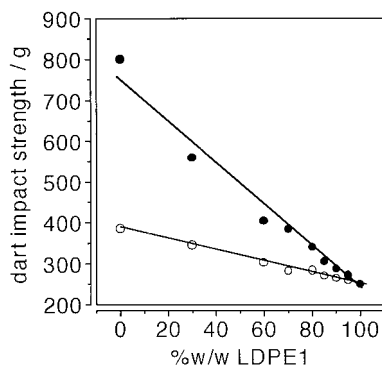


Figure 2 Plots of the dart impact strength versus the blend composition for the B1 blend systems: (○) B1(a) system and (●) B1(b) system.

behavior. Figure 2 shows a plot of the dart impact strength versus the blend composition for these systems. The dart impact strength has been chosen as a typical example of a physicochemical parameter that is expected to exhibit linear variation with the blend composition in idealized systems.^{34–37} Indeed, such behavior is observed in both of the B1 systems, in which the dart impact strength of each system decreases linearly with increasing LDPE.

In each of the B1 systems, the LDPE1 component is unstabilized, whereas the LLDPE and mLLDPE1 components each contain a certain level of a phenolic AO (see Table II). Therefore, the level of AO in the B1 systems decreases linearly with increasing LDPE1 content. It has been shown that OIt varies linearly with phenolic AO content²⁸ and so in the absence of any adverse effects caused by blend incompatibility, the stability of the B1 systems is expected to vary linearly with the composition. Figure 3 shows a plot of the CL-OIt versus the blend composition for each of the B1 systems. In both cases, the CL-OIt decreases linearly with increasing LDPE1 in the blend, confirming the idealized behavior and suggesting blend compat-

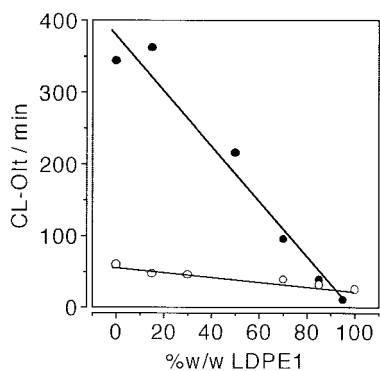


Figure 3 Plots of CL-OIt versus the blend composition for the B1 systems: (○) B1(a) system and (●) B1(b) system. The data were obtained from CL instrument #1. The samples were oxidized under an oxygen atmosphere (1 bar; flow rate = 100 mL min⁻¹) at 170°C.

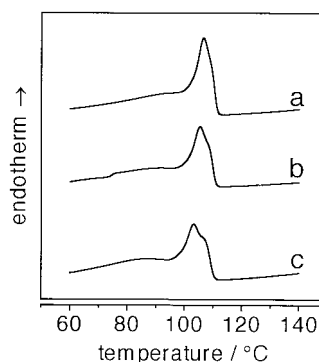


Figure 4 DSC endotherms of selected blends belonging to the B2(a) system. The blends contained (a) 10, (b) 25, and (c) 50% (w/w) mLLDPE2 in LDPE2.

ibility. The data also suggest that the oxidative stability of pure mLLDPE1 is more than six times greater than that of pure LLDPE, although the level of AO in mLLDPE1 is only twice that in LLDPE. Notwithstanding the fact that the efficiency of a given stabilizer is dependent on the polymer matrix in which it is placed, the apparent greater inherent stability of mLLDPE1 may be partly attributable to its more uniform distribution of SCB compared with that of LLDPE.

The stability of commercial LLDPEs is very much affected by the content of the catalyst residue and the chemical structure of the residue. These are, in turn, determined by postpolymerization treatment processes such as deashing, neutralization, or killing. The superior oxidative stability of mLLDPE1 observed in this study can be attributed in part to the clean synthesis involved in its production, which leaves little catalyst residue behind in the polymer.¹ In polymers produced by the more standard Ziegler–Natta and Phillips processes, these metal residues have been shown to catalytically decompose polymer hydroperoxides during the low-temperature oxidation of the polyolefin.¹ Furthermore, it has been shown that in the absence of AOs, LLDPE is much more stable than LDPE.²⁸ The inferior oxidative stability of LDPE has been attributed to its irregular branched structure, which gives rise to labile tertiary hydrogen atoms on its backbone.²⁸ These have been identified as the premier sites for oxygen addition to polymers, leading to hydroperoxide formation and the subsequent degradation of the polymer.³⁸

The melting behavior of each of the quench-cooled B2 systems is similar to that observed for the quench-cooled B1 systems in so far as a single melting endotherm is obtained on the first heat cycle (see Fig. 4). For comparison with these data, Figure 5 shows the variation of the tensile yield strength with the blend composition. Although the observed relationship between the tensile yield strength and the blend composition revealed in Figure 5 is not simple and is not linear,

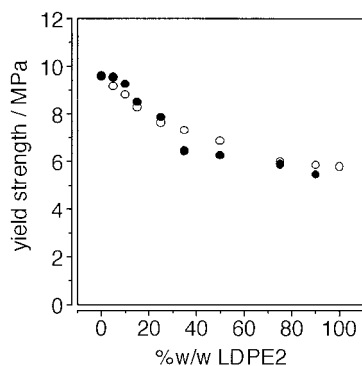


Figure 5 Plots of the tensile yield strength versus the blend composition for the B2 blend systems: (●) B2(a) system and (○) B2(b) system.

there is an apparent smooth trend with no discontinuities, and this is consistent with there being blend compatibility.^{37,39,40}

In the B2 systems, the LDPE2 component is unstabilized, whereas the mLLDPE2 and mLLDPE3 polymers contain a phenolic AO (see Table II). The level of AO in the B2 blends, therefore, decreases linearly with increasing LDPE2. Figure 6 shows a plot of the CL-OIt versus the blend composition for each of the B2 systems. In both cases, the CL-OIt decreases linearly with an increasing concentration of LDPE2 in the blend, and this suggests that the systems exhibit idealized behavior and that each blend is compatible across all compositions. The oxidative stability of pure mLLDPE2 is approximately twice that of the pure mLLDPE3, although these materials contain the same level of AO. A distinguishable difference between the pure resins, however, is the molecular weight, with the lower molecular weight resin (mLLDPE3) exhibiting a lower CL-OIt than the higher molecular weight resin (mLLDPE2). Similarly, the pure LDPE1 and LDPE2 resins have different molecular weights, with the

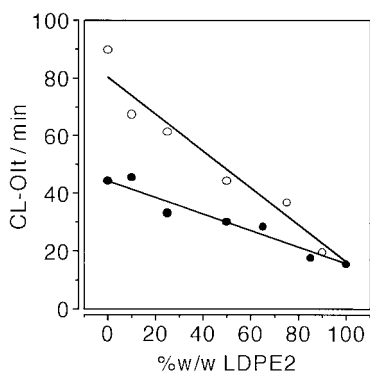


Figure 6 Plots of CL-OIt versus the blend composition for the B2 systems: (●) B2(a) system and (○) B2(b) system. The data were obtained from CL instrument #1. The samples were oxidized under an oxygen atmosphere (1 bar; flow rate = 100 mL min⁻¹) at 170°C.

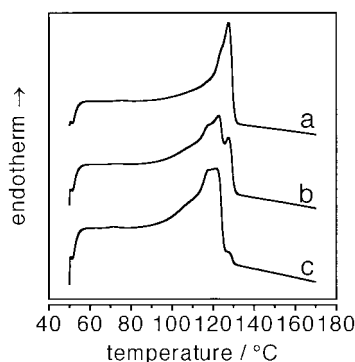


Figure 7 DSC endotherms of selected blends belonging to the B3 system. The blends contained (a) 10, (b) 50, and (c) 90% (w/w) mLLDPE1 in LLDPE.

lower molecular weight resin (LDPE2) exhibiting a slightly lower CL-OIt than LDPE1 (see Figs. 3 and 6).

The B3 system consists of polymers that are structurally similar to each other and that should, therefore, be compatible. The melt compatibility for the components of the B3 system is reflected by a single DSC melting endotherm that is observed for each blend (see Fig. 7), and the assertion of melt compatibility is further supported by the data in Figure 8, which show that the variation of the dart impact strength with the blend composition is linear. Each of the resins that comprise the B3 system is stabilized with a phenolic AO, and the mLLDPE1 resin contains twice the level of AO as the LLDPE1 resin. The total AO level in the blends, therefore, increases linearly with an increasing concentration of LLDPE1. Figure 9 shows a plot of the CL-OIt versus the blend composition for the B3 system, in which the CL-OIt is observed to increase linearly with an increasing concentration of mLLDPE. The linearity of this plot supports the notion that the blend compatibility suggested by the physicochemical and thermal property data (see Figs. 7 and 8) is also reflected in the idealized behavior of the thermo-oxidative stability data.

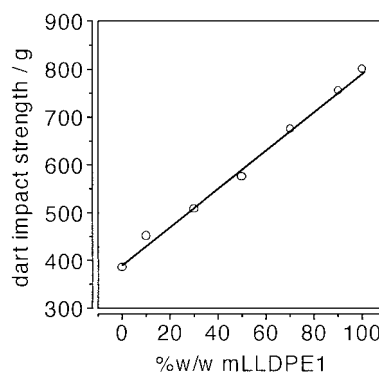


Figure 8 Plot of the dart impact strength versus the blend composition for the B3 system.

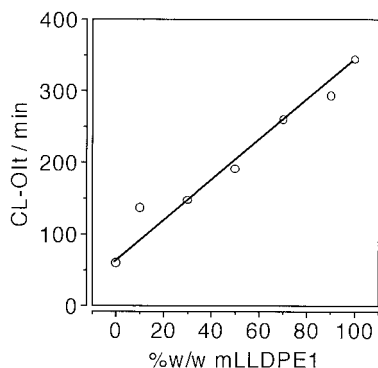


Figure 9 Plot of CL-OIt versus the blend composition for the B3 system. The data were obtained from CL instrument #1. The samples were oxidized under an oxygen atmosphere (1 bar; flow rate = 100 mL min⁻¹) at 170°C.

Nonidealized systems

The B4 systems in which mLLDPE4 is blended with either HDPE1 or HDPE2 are less ideal.

Figure 10 shows the DSC melting endotherms for selected blends belonging to the B4(a) system, in which two peaks covering a wide melting range are evident and correspond to the blend components. Indeed, the endothermic curves for all blend systems studied in this work cover a notably wide melting range. However, endothermic curves showing a significantly wider melting range and multiple peaks when compared with those of the individual polymers have been interpreted as being indicative of immiscibility in the blend. The behavior of the B4(b) system is similar to that of the B4(a) system, with two peaks distinguishable in each endotherm. The presence of two distinct peaks in the endotherms suggests that some degree of immiscibility exists in the melt and that the components in these systems are incompatible. The incompatibility exhibited in the thermal data is also reflected in the various physicochemical properties of the blends, most notably in the Izod impact strength (see Fig. 11), which varies nonlinearly

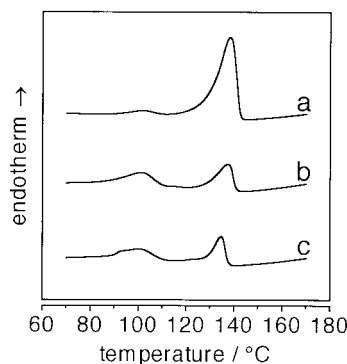


Figure 10 DSC endotherms of selected blends belonging to the B4(a) system. The blends contained (a) 10, (b) 50, and (c) 85% (w/w) mLLDPE4 in HDPE1.

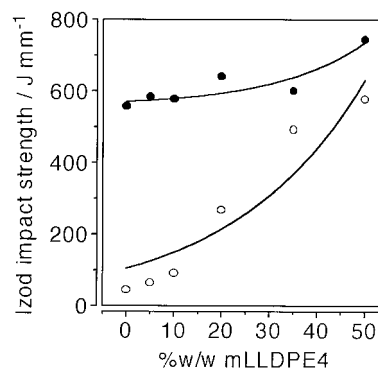


Figure 11 Plots of the Izod impact strength versus the blend composition for the B4 blend systems: (●) B4(a) system and (○) B4(b) system.

with the blend composition such that the deviation is less than the theoretical additive.⁴¹

Each of the mLLDPE4, HDPE1, and HDPE2 components of the B4 systems contain a phenolic AO so that mLLDPE4 is stabilized at a relatively higher level than either HDPE1 or HDPE2 (see Table II). The overall level of AO in each system, therefore, increases linearly with an increasing mLLDPE4 level. Figure 12 shows a plot of the CL-OIt versus the blend composition for each of the B4 systems. In contrast to the other systems studied in this work, the CL-OIt of each of the B4 systems does not increase linearly with an increasing level of the more stable component in the blend. The CL-OIt values of the B4(a) system deviate negatively from the theoretical straight line drawn between the OITs of the pure components (i.e., the theoretical line that represents the situation in which the observed stability is additive).

It is important to note that because the activation energy for thermal oxidation is typically high for stabilized samples, small differences in temperature will give rise to large deviations in the observed OIt. How-

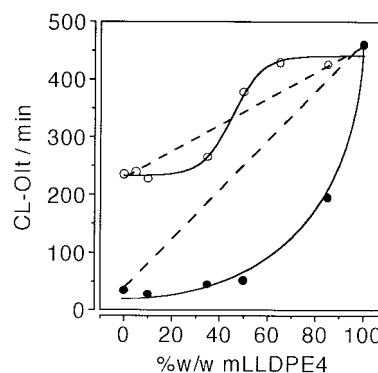


Figure 12 Plots of CL-OIt versus the blend composition for the B4 systems: (●) B4(a) system and (○) B4(b) system. The data were obtained from CL instrument #1. The samples were oxidized under an oxygen atmosphere (1 bar; flow rate = 100 mL min⁻¹) at 170°C. The dotted lines show expected trends for idealized behavior.

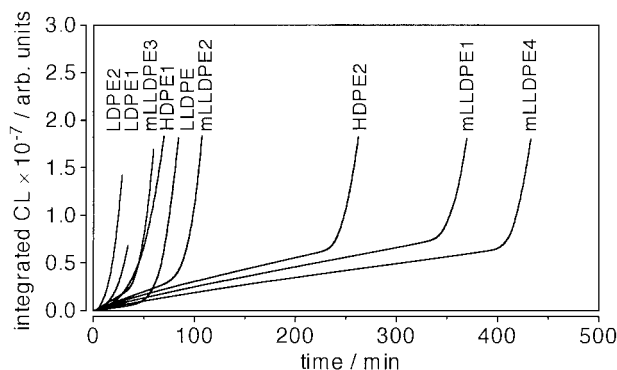


Figure 13 Integrated CL profiles obtained from CL instrument #2 for each of the commercial PE resins used to make the blends.

ever, the consistent trends exhibited by the OIt values obtained in this work suggest that such temperature fluctuation effects are not responsible for the observed deviations from idealized behavior. Indeed, the deviation of the B4(a) system is negative for all compositions in the entire range. In the case of the B4(b) system, the deviation is negative only up to a composition of about 40% (w/w) mLLDPE, after which the CL approaches that of the pure mLLDPE4. The persistence of a negative deviation for the B4(a) system across all compositions suggests that this system is less compatible than the B4(b) system. In either case, the CL-OIt behavior is nonideal, and this is a reflection of the behavior previously observed in the other standard tests (see Figs. 10 and 11). Furthermore, similar nonlinear OIt behavior with the blend composition has been observed for incompatible blends of ethylene-propylene rubber (EPR) and PP.⁴² In the B4 systems studied in this work, the similarly observed effects may be due to a decreased stabilizer efficiency that occurs when the solid-state incompatibility of the blend components persists to produce a melt that is heterogeneous. The heterogeneity of the resultant melt may, therefore, play a key role in the decreased stabilizer efficiency that is observed.

Consistency between the CL instruments and techniques

For the assessment of the consistency of CL-OIt data obtained from two different instruments, each of the nine commercial PE formulations that were used to make the blend systems depicted in Table III were oxidized in CL instrument #2 under the same conditions used previously for CL instrument #1 (i.e., 170°C, oxygen atmosphere, 1 bar, flow rate = 100 mL min⁻¹). Shown in Figure 14 are the integrated CL profiles obtained from CL instrument #2 for each of the PE resins. The mLLDPE1 and mLLDPE4 resins are the most stable, presumably because of the high level of

AO in each. The low stabilities of mLLDPE2 and mLLDPE3 may partly be attributed to their low molecular weight, as reflected by their high MI₂ values (see Table II). The structural uniformity²⁸ and the absence of catalyst residues in metallocene-catalyzed PE resins¹ are believed to contribute to the stability of these materials, and the relative order of inherent stability of PE resins has been reported by other workers as mLLDPE > HDPE > LDPE.^{1,28} However, in this study, it is unlikely that the effects of structural differences between the metallocene-catalyzed resins outweigh those due to the respective stabilizer levels, and so the relative order of stability observed among the resins is most likely to have been determined by the level of AO in each resin. In particular, the AO content of HDPE2 lies between that of mLLDPE1 and mLLDPE4, and this is reflected by its intermediate stability; however, the inherent stability of HDPE2 is also determined to some extent by its high degree of crystallinity, which inhibits oxygen access during oxidation.²⁸ The LDPE resins exhibit the lowest stability, and this is presumably due the absence of a stabilizer in these and, to some extent, their low crystallinities. Similarly, the lower stability of HDPE2 compared with that of HDPE1 is also attributable to the relative AO levels in these materials.

An indication of the consistency of typical CL-OIt data can be achieved by the plotting of the CL-OIt data that were obtained with CL instrument #1 against the corresponding data that were obtained with CL instrument #2. Figure 14 shows such a plot in which the CL-OIt values plotted on the abscissa and ordinate axes were derived from the integrated CL profiles by means of the STD analysis protocol described previously.³¹ The linearity of the plot suggests that there is a high degree of consistency between the results obtained from the two instruments, and the favorable gradient and intercept values, which are close to unity and zero, respectively, further suggest that a high degree of reproducibility has been attained.

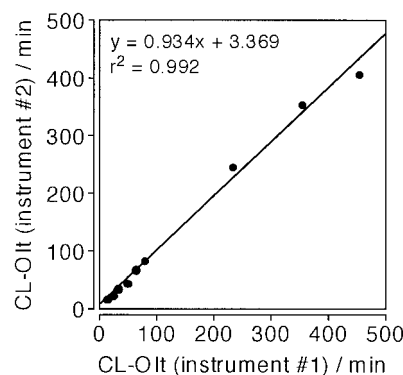


Figure 14 Plots of CL-OIt values obtained from CL instrument #2 versus the corresponding CL-OIt values obtained from CL instrument #1 for each of the commercial PE resins used to make the blends.

A preliminary investigation of the extent to which results obtained from CLI experiments correlate with those obtained from photon-counting CL experiments was conducted with four of the pure resins that were used to make the blends. These resins were individually subjected to oxidation in a CLI apparatus under the same conditions used for the single-photon counting CL studies (i.e., 170°C, oxygen atmosphere, 1 bar, flow rate = 100 mL min⁻¹). Figure 15 shows the integrated CLI profiles for these resins together with the indicated CLI-OIt values that were obtained with STD analysis.³¹ The CLI experiments were conducted with single samples to prevent the possible inter-sample infection observed previously during multiple sample CLI experiments.^{43,44} The order of stability that is revealed by the results of the CLI experiments is the same as that observed previously in the single-photon-counting experiments, although the CLI-OIt values are significantly greater than the corresponding CL-OIt values. A more quantitative assessment of the correlation between the two techniques can be made by the plotting of the CL-OIt values obtained from the single-photon-counting experiments against the CLI-OIt values obtained from the CLI experiments. Such plots are presented in Figure 16 for CL-OIt data derived from both CL instrument #1 and CL instrument #2. The plots show that, for each single-photon-counting instrument, there is a good correlation between the OIt values obtained with it and those obtained with the CLI instrument. However, there is an offset of approximately 100 min with respect to the CLI data that is attributable to a discrepancy in the temperature calibration of the CLI instrument during these preliminary trials. This highlights the importance of accurate temperature calibration in CL work.

CONCLUSIONS

The technique of CL monitoring can be applied successfully to polymer blends involving polyolefins and,

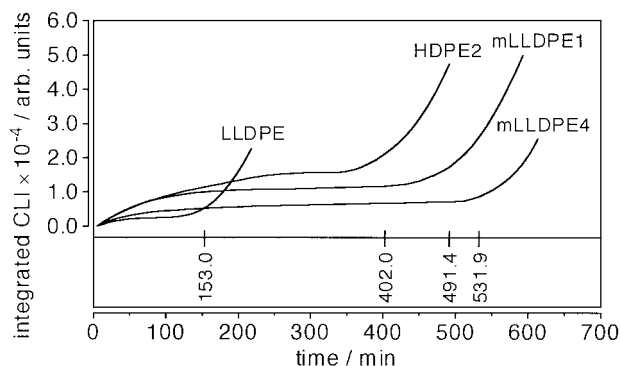


Figure 15 Integrated CLI profiles for selected PE resins that were oxidized at 170°C under an oxygen atmosphere (1 bar; flow rate = 100 mL min⁻¹).

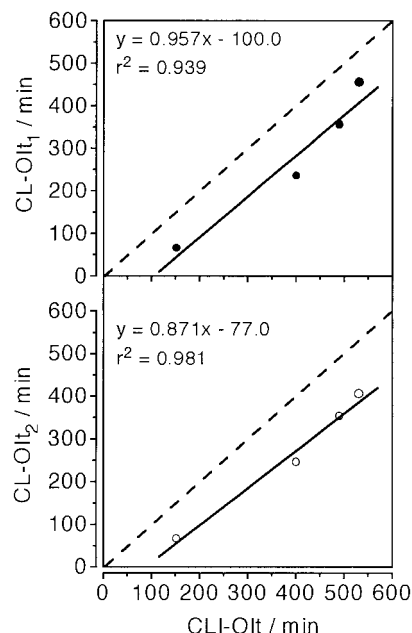


Figure 16 Comparison of CL-OIt data obtained from single-photon-counting CL experiments with CLI-OIt data obtained from CLI experiments. The CL-OIt data were obtained with two different instruments: (●) CL instrument #1 and (○) CL instrument #2. The broken lines indicate the desirable situation in which total correlation exists.

in particular, blends containing metallocene-catalyzed PE. The CL data obtained for the blends are consistent with the thermal and physicomechanical properties of the blends, and the CL technique has the potential to produce information on important aspects of blends such as the blend miscibility. Decreased blend miscibility is reflected in the CL data as a departure from the idealized behavior that is observed for more miscible blends. Furthermore, in the case of nonideal systems that exhibit immiscibility between the components, it appears that the immiscibility in the solid state is reflected to some extent in the behavior of the melt.

The preliminary experiments conducted to determine the level of consistency of CL results with respect to both variability between instruments and variability between techniques indicate that a high degree of correlation exists in each case. However, differences in temperature calibration between CL apparatus can result in an offset in the derived OIt values.

The authors are grateful to Mettler-Toledo for supplying the CL-DSC instrument.

References

1. Foster, G. N.; Wasserman, S. H.; Yacka, D. J. *Angew Makromol Chem* 1997, 252, 11.
2. Gugumus, F. *Polym Degrad Stab* 1996, 52, 131.

3. Gugumus, F. *Polym Degrad Stab* 1996, 52, 145.
4. Gugumus, F. *Polym Degrad Stab* 1996, 52, 159.
5. Gugumus, F. *Polym Degrad Stab* 1996, 53, 161.
6. Gugumus, F. *Polym Degrad Stab* 1997, 55, 21.
7. Allen, N. S.; Edge, M.; Holdsworth, D.; Rahaman, A.; Catalina, F.; Fontan, E.; Escalona, A. M.; Sibon, F. F. *Polym Degrad Stab* 2000, 67, 57.
8. Hussein, I. A.; Ho, K.; Goyal, S. K.; Karbaszewski, E.; Williams, M. C. *Polym Degrad Stab* 2000, 68, 381.
9. La Mantia, F. P.; Valenza, A. *Angew Makromol Chem* 1994, 216, 45.
10. Ghosh, P.; Chattopadhyay, B.; Sen, A. K. *Eur Polym J* 1996, 32, 1015.
11. Ray, I.; Roy, S.; Chaki, T. K.; Khastgir, D. *J Elast Plast* 1994, 26, 168.
12. Waldman, W. R.; De Paoli, M. A. *Polym Degrad Stab* 1998, 60, 301.
13. Matisová-Rychlá, L.; Rychlý, J.; Fodor, Z.; Barabas, K.; Iring, M.; Tudos, F. *Int J Polym Mater* 1990, 13, 227.
14. Khabbaz, F. A. A. *J Appl Polym Sci* 2001, 79, 2309.
15. Matisová-Rychlá, L.; Chodák, I.; Rychlý, J.; Bussink, J. *J Appl Polym Sci* 1993, 49, 1887.
16. Fearon, P. K.; Marshall, N.; Billingham, N. C.; Bigger, S. W. *J Appl Polym Sci* 2001, 79, 733.
17. Kihara, H.; Hosoda, S. *Polym J* 1990, 22, 763.
18. Memetea, T.; Vuluga, Z.; Hagiopol, C. *Int J Polym Mater* 1991, 15, 187.
19. Mendenhall, G. D. *Angew Chem Int Ed Engl* 1990, 29, 362.
20. Zlatkevich, L. In *Polymer Stabilisation and Degradation*; Klemchuk, P., Ed.; ACS Symposium Series 280; American Chemical Society: Washington, DC, 1985; Chapter 27.
21. Mattson, B.; Kron, A.; Reitberger, T.; Craig, A. Y.; Fleming, R. H. *Polym Test* 1992, 11, 357.
22. Fleming, R. H.; Craig, A. Y. *Polym Degrad Stab* 1992, 37, 173.
23. Hosoda, S.; Seki, Y.; Kihara, H. *Polymer* 1993, 34, 4602.
24. Ablblad, G.; Stenberg, B.; Terselius, B.; Reitberger, T. *Polym Test* 1997, 16, 59.
25. Mason, L. R.; Reynolds, A. B. *J Appl Polym Sci* 1997, 66, 1691.
26. Audouin-Jirackova, L.; Verdu, J. *J Polym Sci Part A: Polym Chem* 1987, 25, 1205.
27. Hosoda, S.; Kihara, H. *Annu Tech Conf* 1988, 34, 941.
28. Setnescu, R.; Jipa, S.; Osawa, Z. *Polym Degrad Stab* 1998, 60, 377.
29. Zenjiro, O.; Kenji, T.; Fujiko, K. *Mater Life* 1990, 2, 162.
30. Naito, K.; Kwei, T. K. *J Polym Sci Polym Chem Ed* 1979, 17, 2935.
31. Fearon, P. K.; Whiteman, D. J.; Billingham, N. C.; Bigger, S. W. *J Appl Polym Sci* 2001, 79, 1986.
32. Hill, M. J.; Barham, P. J. *Polymer* 1992, 33, 4099.
33. Hill, M. J.; Puig, C. C. *J Appl Polym Sci* 1997, 65, 1921.
34. Ta demir, M.; Yildirim, H. *J Appl Polym Sci* 2002, 83, 2967.
35. Samios, C. K.; Kalfoglou, N. K. *Polymer* 1998, 39, 3863.
36. Vadhar, P.; Kyu, T. *Polym Eng Sci* 1987, 27, 202.
37. Cho, K.; Lee, B. H.; Hwang, K.-M.; Lee, H.; Choe, S. *Polym Eng Sci* 1998, 38, 1969.
38. Vaillant, D.; Lacoste, J.; Dauphin, G. *Polym Degrad Stab* 1994, 45, 355.
39. Rana, D.; Lee, C. H.; Cho, K.; Lee, B. H.; Choe, S. *J Appl Polym Sci* 1998, 69, 2441.
40. Raue, F.; Ehrenstein, G. W. *J Elast Plast* 1999, 31, 194.
41. Schellenberg, J. *Adv Polym Technol* 1997, 16, 135.
42. Billingham, N. C.; Hoad, O. J.; Chenard, F.; Whiteman, D. J. *Macromol Symp* 1997, 115, 203.
43. Celina, M.; George, G. A.; Lacey, D. J.; Billingham, N. C. *Polym Degrad Stab* 1995, 47, 311.
44. Celina, M.; George, G. A. *Polym Degrad Stab* 1995, 50, 89.
45. Nugay, N.; Tinçer, T. *Eur Polym J* 1994, 30, 473.